Published in final edited form as:
Biochem J. 2013 February 1; 449(3): 661–672. doi:10.1042/BJ20120213.

Sphingosine 1-Phosphate induces filopodia formation through S1P2R activation of ERM proteins

K. Alexa Orr Gandy[1], **Daniel Canals**[1], **Mohamad Adada**, **Masayuki Wada**, **Patrick Roddy**, **Ashley J. Snider**, **Yusuf A. Hannun**, and **Lina M. Obeid**
From the Departments of Molecular and Cellular Biology and Pathobiology (K.A.O.G.), and Biochemistry and Molecular Biology (P.R.), Medical University of South Carolina, Charleston, SC 29425 and The Department of Medicine (D.C., M.A., M.W., Y.A.H. and, L.M.O.), Stony Brook University, Stony Brook, NY 11794 and The Northport VA, Medical Center (A.J.S., L.M.O.), Northport, NY 11768

Abstract

Previously we demonstrated that the sphingolipids ceramide and sphingosine 1-phosphate (S1P) regulate phosphorylation of the ERM family of cytoskeletal proteins [1]. Herein, we show that exogenously applied or endogenously generated S1P (in a sphingosine kinase-dependent manner) result in significant increases in phosphorylation of ERM proteins as well as filopodia formation. Utilizing phosphomimetic and non-phosphorylatable ezrin mutants, we show that the S1P-induced cytoskeletal protrusions are dependent on ERM phosphorylation. Employing various pharmacological S1P receptor agonists and antagonists, along with small interfering RNA techniques and genetic knockout approaches, we identify the S1P Receptor 2 (S1P2R) as the specific and necessary receptor to induce phosphorylation of ERM proteins and subsequent filopodia formation. Taken together, the results demonstrate a novel mechanism by which S1P regulates cellular architecture that requires S1P2R and subsequent phosphorylation of ERM proteins.

Introduction

The ERM family of proteins, Ezrin (82KDa), radixin (80KDa) and moesin (75KDa), links the plasma membrane with the actin cortical cytoskeleton, and plays a role in regulating cell morphology, cell polarization, and formation of plasma membrane protrusions such as filopodia and lamellipodia [2]. ERM proteins also work as scaffolding proteins for a growing list of plasma membrane and cytoskeletal proteins with roles in cell signal transduction, communicating with the extracellular matrix and with surrounding cells [3]. The study of the ERM family of proteins has captured significant interest as its members have been strongly related to an increasing number of cancers, including lung [4], colon [5] and breast cancers [6]. The role of ezrin in cancer has been attributed to the 1) binding and

Corresponding author: Lina M. Obeid, M.D Department of Medicine, Stony Brook University. Health Science Center, L-4, 179, Stony Brook, NY 11794-8430. Lina.Obeid@stonybrookmedicine.edu.
[1]These authors contributed equally to this work and are considered co-first author
Reprint requests should be sent to: Lina M. Obeid, M.D., Department of Medicine, Stony Brook University. Health Science Center, L-4, 179, Stony Brook, NY 11794-8430. Lina.Obeid@stonybrookmedicine.edu

Author Contributions
Participated in research design: K. Alexa Orr Gandy, Daniel Canals, Yusuf A. Hannun and Lina M. Obeid
Preparation of analytic tools: Daniel Canals, Ashley J. Snider, Masayuki Wada, Patrick Roddy
Conducted experiments: K. Alexa Orr Gandy, Daniel Canals and Mohamad Adada
Performed data analysis: K. Alexa Orr Gandy, Daniel Canals
Wrote or contributed to the writing of the manuscript: K. Alexa Orr, Daniel Canals, Yusuf A. Hannun and Lina M. Obeid
K. Alexa Orr Gandy and Daniel Canals contributed equally and are considered co-first authors

recruitment of plasma membrane receptors and other proteins such as FasL receptor (CD95) [7], hyaluronan receptor (CD44) [8], Na^+/H^+ exchanger-1 (NHE1) [9], cadherins [10], integrins [11], tumor suppressor protein merlin (NF2) [12] and others, most of which are also implicated in cancer progression [13] and 2) promoting filopodia and lamellipodia formation, enhancing migration, invasion of surrounding tissues, and adhesion to new metastatic settlements [14].

The activation of ERM proteins is regulated by a change in protein conformation. In the inactive (closed) conformation, the amino-terminus (N-ter) and the carboxyl-terminus (C-ter) interact with each other, and the ERM proteins remain soluble in the cytosol. Activation of ERM proteins requires N-ter binding to plasma membrane phospatidylinositol 4, 5 bisphosphate (PIP2) and phosphorylation of a conserved carboxy-terminal threonine (ezrin Thr^{567}, radixin Thr^{564}, and moesin Thr^{558}). Phosphorylation of the conserved Thr creates a steric restriction between the C-ter and the N-ter, which therefore cannot interact with each other, leading to the active (open) conformation. In this conformation, the N-ter interacts with the plasma membrane, and the C-ter interacts with the actin cortical cytoskeleton. Little is known about the control of ERM activation, although a few protein kinases have been reported to phosphorylate ERM *in vivo* (conventional and atypical PKC [4], protein Rho kinase [12], G protein-coupled receptor kinase 2 (GRK2) [15], myotonic dystrophy kinase-related Cdc42-binding kinase [16], and Nck-interacting kinase [17], and only a couple of growth factors are known to activate ERM proteins. Epidermal growth factor (EGF) [18] and platelet-derived growth factor (PDGF) have been reported as effectors that lead to ERM phosphorylation and activation [17].

Our group demonstrated that ERM family of proteins were acutely regulated by acid sphingomyelinase [19], and more directly by the interconversion of the sphingolipids ceramide and sphingosine-1-phosphate (S1P) [1]. Ceramide has been widely associated with senescence, cell cycle arrest, and apoptosis [20], and it was observed that ceramide induced dephosphorylation of ERM proteins. On the other hand, S1P, which has a role in enhancing inflammation, cell survival and cell migration [20], was found to dramatically induce phosphorylation of ERM proteins [1]. Interestingly, both ERM proteins and S1P have been found to be up-regulated in some cancers [2, 21].

In the cell, S1P is formed by phosphorylation of sphingosine by one of two sphingosine kinases (SK1, 2) and exported outside the cell whereby it can activate different receptors in an autocrine or paracrine manner. The pleiotropic effects of S1P in cells are mostly mediated through its interaction with five G protein-coupled receptors (GPCR), namely S1P1R-S1P5R which activate varying combinations of G-proteins [20]. The finding of significant ERM phosphorylation in response to S1P prompted us to determine if a specific SK isoform was involved, what S1P receptors were involved in the process, and if this resulted in activation of ERMs and induction of ERM-mediated responses.

In this study, we found that S1P when exogenously applied or endogenously generated predominantly by the action of SK1 resulted in activation of ERM proteins leading to filopodia formation preferentially through activation of S1P receptor 2 (S1P2R). Using a combination of S1P-receptor agonists and antagonists, as well as using small interference RNA technology and knockout mice, we found that filopodia formation upon S1P treatment was phospho-ERM dependent. This was confirmed by using ezrin phospho-mimetic and non-phosphorylatable mutants. The implications of these results are discussed.

Materials and Methods

Materials

High glucose Dulbecco's modified Eagle's medium (DMEM), fetal bovine serum (FBS), penicillin-streptomycin, rhodamine-phalloidin and Superscript III First-Strand Synthesis kit were purchased from Invitrogen (Carlsbald, CA). Essentially fatty acid free bovine serum albumin (BSA), and monoclonal anti-GAPDH antibody were from Sigma-Aldrich (St. Louis, MO). D- *erythro*-sphingosine 1-phosphate (S1P) and D-*erythro*-sphingosine (Sph) were from Avanti polar lipids (Alabaster, AL). Anti-phospho ERM, anti-moesin, and anti-phospho ERK antibodies were from Cell Signaling Technology (Danvers, MA). Anti VSV-G and HRP-labeled secondary antibodies were from Santa Cruz Biotechnology (Santa Cruz, CA). Chemiluminescence kit was from ThermoScientific (Suwanee, GA). Draq5 was purchased from Alexis Biochemicals (San Diego, CA). SYBR Green was purchased from Bio-Rad (Hercules, CA). SEW-2871, JTE-013, BML-241 and FTY720-P were purchased from Cayman Chemical (Ann Arbor, MI). S1P2R-GFP plasmid DNA was purchased from Origene (Rockville, MD). Sphingosine Kinase 1 inhibitor, SKX, was kindly provided by Sphynx Therapeutics (Charlottesville, VA).

Cell lines and Culture Conditions

HeLa cells were originally purchased from American Type Culture Collection (ATCC, Manassas, VA). Cells were maintained in DMEM supplemented with 10% FBS and 1% penicillin-streptomycin and incubated in standard culture conditions: 37 C, and 5% CO2 When FBS free medium was used, medium was supplemented with 0.1% BSA, 1% penicillin-streptomycin and 10mM HEPES. In all cases, prior to experimentation, cells were serum starved overnight (16–18h) when approximately 75% confluent.

Generation of Mouse Embryonic Fibroblasts

S1P2R mice were a kind gift from Dr. Richard L. Proia (National Institutes of Diabetes and Digestive and Kidney Disease, National Institutes of Health, Bethesda, MD). MEFs were generated from S1P2R+/− littermate matings in a C57BL6.129S background. MEFs were isolated from E13.5 embryos. Cells were maintained in high glucose DMEM supplemented with 10% FBS in standard culture conditions. For genotyping, genomic DNA was extracted using DNeasy Blood and Tissue kit (Qiagen) and 2μl of DNA was combined with 1μl each of either S1P2R primer 1 and S1P2R primer 2 or S1P2R primer 1 and the NEO primer. This was combined with 21μl of PCR Platinum SuperMix (Invitrogen) for a total reaction volume of 25μl for PCR. The following primers (10μM) from Integrated DNA Technologies (Coralville, IA) were used for the detection of the wild-type or knockout S1P2R: S1P2R primer 1 5′-GCAGTGACAAAAGCTGCCGAATGCTGATG-3′, S1P2R primer 2 5′-AGATGGTGACCACGCAGAGCACGTAGTG-3′, and NEO primer 5′-TGACCGCTTCCTCGTGCTTTACGGTATCG-3′. PCR was performed on a Biometra Thermocycler T3000 with the following reaction conditions: 95 °C for 0.5 min; 55 °C for 0.5 min; 72 °C for 0.5 min for 40 cycles. PCR products were run separately for each set of primers on a 1.5% Agarose gel and visualized by UV transillumination. A 170bp band indicated the WT S1P2R allele and a band at 220bp represented a knockout or NEO allele.

Immunoblotting

Immunoblotting was performed as previously described [1]. Following removal of media, cells were immediately lysed in buffer containing 1% (w/v) SDS. Following harvest, cells were sonicated and boiled before proteins were separated via SDS-PAGE (10%, Tris-HCl) using the Bio-Rad Criterion system. Proteins were transferred to nitrocellulose membranes and blocked for at least 1 h with 5% nonfat milk in PBS/0.1% Tween 20 (PBS-T).

Membranes were then incubated with primary antibody diluted 1:000 (pERM, t-Moe, VSVG and pERK) or 1:6000 (GAPDH) at 4°C overnight. Secondary antibody incubation and visualization were carried out following the manufacturer's protocol.

RNA Interference

Gene silencing was carried out using siRNA, purchased from Qiagen (Valencia, CA), directed against human SK1, SK2 and S1P2R: SK1, 5′-AAGGGCAAGGCCTTGCAGCTC-3′; SK2, Hs_SPHK2_5 FlexiTube siRNA SI00288561 (FlexiTube siRNA, Experimentally verified, Qiagen); S1P2R, Hs_EDG5_6 FlexiTube siRNA SI02663227 (FlexiTube siRNA, Experimentally verified, Qiagen). Scrambled siRNA was used as a negative control: SCR, Negative control siRNA (1027130, Qiagen). Transfections were carried out according to manufacturer's protocol, using Qiagen HiPerFect transfection reagent. Briefly, HeLa cells were seeded into 6-well plates (~200,000 cells/well) and treated with 20nM siRNA using Qiagen's fast-forward transfection protocol for adherent cells. Following 24 h of siRNA treatment, fresh media was added. Experiments were carried out 24 h following replacement of media, 48 h after siRNA transfection

Real Time Reverse Transcriptase-PCR (RT-PCR)

RNA was harvested from cells using QIAShredder and RNeasy kits from Qiagen. RNA concentration was assessed by measuring absorbance at 260 nm. 1ug of RNA was converted to cDNA using SuperScript III First-Strand Synthesis Systems from Invitrogen. cDNA was diluted 1:10 and 5 μL was used per 25μL reaction. Each 25 μL RT-PCR contained a ratio of 12.5: 0.5: 0.5: 6.5 (SYBR Green: forward primer, 10 μM: reverse primer, 10 μM: dH_2O). Using a Bio-Rad iCycler, reactions detecting expression of human genes were carried out as previously explained [22]. Briefly, following 3 minutes at 95°C, 40 cycles of 1)10s melt at 95 °C, 2) 45s annealing at 54 °C, and 3) 45s extension at 68 °C were carried out. Reactions detecting mouse gene expression were carried out as described above; however the annealing was performed at 60 °C. The following primers sequences were used to detect expression: human β-actin forward (hβ-actin F), 5′-ATTGGCAATGAGCGGTTCC-3′ ; hβ-actin reverse (hβ-actin R), 5′-GGTAGTTTCGTGGCCACA-3; hSK1 F, 5′-CTGGCAGCTTCCTTGAACCAT-3′; hSK1 R, 5′-TGTGCAGAGACAGCAGGTTCA-3′; hSK2 F, 5′-TTGCTCAACTGCTCACTG-3′; hSK2 R, 5′-AGACAGGAAGGAGAAACAG-3′; hS1P1R F, 5′-TGCGGGAAGGGAGTATGTTTG-3′; hS1P1R R, 5′-AGGAAGAGGCGGAAGTTATTGC-3′; hS1P2R F, 5′-CCCAACAAGGTCCCAGGAACAC-3′; hS1P2R R GCAACAGAGGATGACGATGAAGG-3′; hS1P3R F, 5′-AACAATAGCACGCACTCTCC-3′; hS1P3R R, 5′-ATAAGAACACAGCCGGACAG-3′; hS1P4R F, 5′-TGGTGGTGCTGGAGAACTTG-3′; hS1P4R R, 5′-TGATGTTCACCAGGCAATAGTAG-3′; hS1P5R F, 5′-AAATGTGCCCATGTGTTCTAAGAAATG-3′; hS1P5R R, 5′-AACTACTCCTTCAGCTCC-3′; mouse β-actin forward (mβ-actin F), 5′-CGGGACCTCACAGACTACCTC-3′; mβ-actin R, 5′-AACCGCTCGTTGCCAATA-3′; mS1P1R F, 5′-CTCCACCGTGCTCCCGCTCTA-3′; mS1P1R R, 5′-GGAGATGTTCTTGCGGAAGGTCAGG-3′; mS1P2R F, 5′-GCGTGGTCACCATCTTCTCC-3′; mS1P2R R, 5′-CGTCTGAGGACCAGCAACATC-3′; mS1P3R F, 5′-CATCGCCTTCCTCATCAGTATCTTC-3′; mS1P3R R, 5′-CACAATCACTACGGTCCGCCA-3′; mS1P4R F, 5′-GCACCTTGAGCATAACAGGA-3′; mS1P4R R, 5′-CGGGGACAGACTGAGAGAGG-3′; mS1P5R F, 5′-ACTGCTTAGGACGCCTGGAA-3′; mS1P5R R, 5′-

CCGCACCTGACAGTAAATCCTT-3′. Using Q-Gene software [22], threshold cycle (C_t) values were normalized to β-actin and displayed as mean normalized expression.

Immunofluorescence and Confocal Microscopy

Immunofluorescence and laser-scanning confocal microscopy analysis was carried out as previously described with minor modifications [1]. HeLa cells were plated onto poly-d-lysine coated 35mm confocal dishes (MatTek Corporation). The following day, cells were serum starved overnight prior to being exposed to treatments. Cells were fixed using paraformaldehyde, washed and permeabilized with 0.1% Triton X-100. Cells were blocked in 2% human serum and incubated with primary antibodies (1:200) in 2% serum overnight. Secondary antibody incubation was carried out per manufacturer protocol. Using a LSM510 META confocal microscope (Carl Zeiss, Inc.), images were obtained then analyzed using free downloadable LSM Image Browser Software (www.Zeiss.com).

Plasmid Constructs and Transient Transfections

Full-length ezrin cDNA, VSV-G tag pCB6 plasmid has been previously described [19]. Single mutation on ezrin T567D and T567A were generated using QuickChange Site-Directed Mutagenesis Kit from Stratagene (La Jolla, CA). All plasmids were sequenced to confirm the sequence in Genewiz (South Plainfield, NJ). Cells, growing on 35 mm dishes, were transfected with 1 μg of pCB6-Ezrin plasmid DNA or 1 μg S1P2R-GFP plasmid using Lipofectamine (Invitrogen) or Effectene Qiagen) transfection reagent (according to the manufacturer's instructions.

Cellular Invasion Assays

Cell invasion studies were carried out using the BD Biosciences Tumor Invasion System (345166) according to manufacturer's protocol, with minor changes. Briefly, following serum starvation for ~4 hours, cells were trypsinized, washed twice with serum free (SF) media then resuspended at 200,000 cells/mL in SF media. 750μL appropriate media or media plus chemo attractant was placed in the well of a 24-well plate, followed by 500μL cell suspension in SF media, plus or minus 5μM JTE013, in the apical chamber of the trans well insert. Cells were allowed to invade under normal cell culture conditions for 48h. After 48h, 500μL Calcein AM was added to wells of a fresh 24-well plate per manufacturer's protocol. Trans well inserts were removed carefully and cells in the apical chamber were wiped away using a cotton swab. Inserts were then added to the Calcein AM and incubated for 1h at 37°C. Cells were visualized under fluorescence microscopy and pictures of each quadrant of the underside of each trans well insert were taken and total invading cells were counted using NIH Image J software.

Results

S1P induces ERM phosphorylation

In order to characterize sphingolipid-mediated activation of ERM proteins we performed time course and dose response studies of S1P treatment on ERM phosphorylation. Treating HeLa cells with 100 nM S1P induced acute and robust phosphorylation of ERM proteins occurred as early as 0.5 minutes and lasted for up to at least 15 minutes (Fig 1A). ERK phosphorylation is well known to occur in response to S1P action on its receptors [23, 24] therefore, ERK was used as a positive control for S1P treatment. Treating HeLa cells with 100 nM S1P induced ERK phosphorylation by approximately two minutes which was short-lived, decreasing after 5 minutes. Next, HeLa cells were treated with increasing concentrations of S1P for 5 minutes. ERM phosphorylation was increased in a S1P-dose dependent manner (Fig 1B); treating cells with as little as 1nM S1P induced robust

phosphorylation of both ERK and ERM. Treating cells with increasing doses of S1P led to intensified ERM phosphorylation, becoming maximal at 100 nM. As described previously, S1P treatment also increased ERK phosphorylation in a dose-dependent manner [25]. These data demonstrate that exogenous S1P is able to induce phosphorylation of ERM proteins rapidly (faster and more robustly than induction of ERK phosphorylation) and at low nanomolar concentrations.

Next and in order to assess the role of endogenously generated S1P, the effect of exogenously added sphingosine with or without knock down of SK was determined [26]. Treatment with exogenous sphingosine, as well as driving the production of sphingosine at the plasma membrane using exogenous enzymes [27] led to SK-dependent generation of intra and extracellular S1P (supplemental figures 1 and 2). HeLa cells were pretreated with siRNA against SK1 or SK2 and as shown in supplemental figure 3 both SK1 and SK2 were significantly knocked down. The SK knock down was followed by treatment with 1 or 5 μM sphingosine for 10 minutes and evaluated for phospho-ERM. Sphingosine induced ERM phosphorylation in control siRNA-treated cells in a dose-dependent manner such that substantial ERM phosphorylation occurred in response to 1μM sphingosine (Fig. 1C, lanes 2 and 3). HeLa cells pretreated with SK1 siRNA showed significantly less ERM phosphorylation in response to sphingosine (Fig. 1C, lanes 4–6), indicating that SK1-generated S1P is required for ERM phosphorylation in response to exogenously applied sphingosine. In contrast, cells treated with SK2 siRNA showed a notable increase in ERM phosphorylation in response to 1 and 5 μM sphingosine (Fig. 1C, lanes 7–9) indicating that SK2 may be only partially involved in generation of S1P and ERM phosphorylation under these conditions. This data is in line with the differential levels of S1P generated by driving the production of sphingosine at the plasma membrane via treatment with exogenous bacterial sphingomyelinase and ceramidase in mouse embryonic fibroblasts generated from WT, $SK1^{-/-}$ or $SK2^{--}$ mice (supplemental figure 2) [27]; while WT and $SK2^{-/-}$ fibroblasts produced high levels of sphingosine and S1P upon treatment with exogenous enzymes, $SK1^{-/-}$ fibroblasts produced high levels of sphingosine yet substantially lower levels of S1P (supplemental figure 2). These data confirm that exogenous S1P, as well as endogenous S1P generated by the action of SK, induce phosphorylation and activation or ERM proteins.

S1P induces ERM phosphorylation and translocation to newly formed filopodia

Next, in order to examine the cellular consequences of S1P-induced ERM phosphorylation laser-scanning confocal microscopy was used. Under basal conditions HeLa cells exhibited very little phosphorylated ERM which existed in a punctate pattern (Fig 2A). Treating HeLa cells with 10 nM S1P for 10 minutes induced ERM phosphorylation and localization to newly formed filopodia. This is visualized in figure 2B by F-actin staining (red) and phospho-ERM staining (green) both of which localized to newly-formed cytoskeletal processes, consistent with filopodial protrusions (Fig 2B). In order to better visualize phospho-ERM localization and filopodial protrusions, insets in figure 2 show magnified areas of interest. Taken together, these results demonstrate that S1P-induced phospho-ERM is sufficient to induce the organization of filopodial protrusions.

Ezrin phosphorylation is necessary for S1P-induced filopodia formation

Based on the above results, it became important to evaluate if ERM proteins are involved in S1P-mediated filopodia formation. C-terminal phosphorylation of threonine 567, 563 and 558 of ezrin, radixin and moesin, respectively has been shown to be important in ERM activation [28]; therefore, three different ezrin mutant constructs were utilized. Wild type (WT) ezrin, a non-phosphorylatable ezrin mutant and a phospho-mimetic ezrin mutant into a VSV-G vector were overexpressed in HeLa cells. The non-phosphorylatable ezrin mutant contains a threonine 567 to alanine (T567A) mutation, rendering it unable to be

phosphorylated at the conserved, activating threonine residue [29]; while, the phospho-mimetic ezrin mutant contains a threonine 567 to aspartic acid (T567D) mutation which maintains ezrin in an open, active conformation [29]. Confocal microscopy was used to visualize total ezrin (VSV-G tag, green), F-actin (phalloidin, red) and nuclei (DRAQ5, blue) in control and S1P-stimulated cells. Under basal conditions, cells expressing WT-ezrin-VSV-G showed ezrin to be localized predominantly in the cytoplasm; however, stimulation with 10nM S1P prompted remodeling of the actin network along with redistribution of ezrin to the plasma membrane and cellular processes, consistent with filopodia (Fig 3A, B). Similarly, non-treated cells overexpressing the T567A non-phosphorylatable ezrin mutant displayed ezrin located in the cytoplasm; however in these cells S1P treatment failed to induce translocation of T567A-ezrin-VSV-G to the plasma membrane (Fig 3C, D). Importantly, as seen in figure 3D with phalloidin staining (F-actin, red), treating T567A-ezrin-VSV-G-expressing cells with 10nM S1P did not lead to rearrangement of the actin network nor to the formation of cellular processes. These results suggest that ezrin phosphorylation is required for S1P-mediated cytoskeletal rearrangement and filopodia formation and that the TA mutant acts in a dominant negative fashion. In contrast, cells expressing the T567D phospho-mimetic ezrin construct displayed ezrin localized to complex plasma membrane protrusions even under basal conditions (Fig 3E), and treatment with S1P did not induce further formation of cellular processes (Fig 3F). These findings, taken together, provide strong evidence that ezrin phosphorylation is required for S1P-induced cytoskeletal rearrangement and filopodia formation.

S1P induces phosphorylation of ERM proteins via $S1P_2$

Having established that S1P induces phosphorylation of ERM proteins and this phosphorylation event is required for S1P-induced cytoskeletal rearrangement and filopodia formation, we were interested in determining the mechanism by which S1P induces ERM phosphorylation. As mentioned above, S1P can signal through G protein-coupled receptors as well as intracellularly [25] and the expression pattern of S1P receptors in a given cell type largely determines the outcome of S1P treatment. Therefore, we examined S1P receptor expression in the HeLa cells used in our experiments (supplemental figure 4). In the current study we were able to detect the presence of all five S1P receptors; of note, the expression levels of receptors cannot be compared to one another due to potential differences in primer efficiencies. Given the low doses and short times at which S1P is capable of phosphorylating ERM (Fig 1), we first evaluated the possible role of S1P receptors in this process by relying on well characterized pharmacological approaches. HeLa cells were treated with FTY720-P, an agonist for four of the five S1P receptors: S1P1R, S1P3R, S1P4R and S1P5R [30]; in accordance with our previous data, HeLa cells treated with 10nM S1P exhibited a robust increase in ERM phosphorylation, with a concomitant increase in ERK phosphorylation (Fig 4A). On the other hand, while ERK was phosphorylated in response to 10, 100 or 1000nM FTY720-P suggesting that the treatment activated S1P receptors, FTY720-P was unable to induce ERM phosphorylation (Fig 4A). These data appear to rule out S1P receptors 1, 3, 4 and 5 as the main receptors responsible for S1P-mediated ERM phosphorylation. To consolidate evidence that S1P-mediated ERM phosphorylation is S1P1-independent HeLa cells were treated with a specific agonist of the $S1P_1$ receptor, SEW-2871 [31]. While S1P was able to induce phosphorylation of both ERM and ERK, treatment with 1 or 10uM SEW-2871 was only able to phosphorylate ERK suggesting that S1P does not induce ERM phosphorylation via S1P1R (Fig 4B).

We next examined the involvement of S1P3R in S1P regulation of ERM proteins using the S1P3R-specific antagonist BML-241 [32]. In order to reinforce our data suggesting that S1P-induced ERM phosphorylation is S1P3R-independent, HeLa cells were pretreated for 1 hour with vehicle, 1 μM or 7.5 μM BML-241 followed by 10 minutes of S1P treatment (Fig

4C). S1P maintained its ability to induce ERM phosphorylation in the presence of a $S1P_3$-specific antagonist, indicating that the S1P3R receptor is not involved in ERM phosphorylation (Fig 4C). In order to assess the role of S1P2R in ERM phosphorylation, we used the S1P2R-specific antagonist [33], JTE-013, and evaluated phospho-ERM following S1P treatment. HeLa cells were pretreated for 1 hour with vehicle, 1 μM or 10 μM S1P2R-specific antagonist and then exposed for 10 minutes to 10nM S1P; phospho-ERM, phospho-ERK and total moesin levels were evaluated via western blot (Fig 4D). JTE-013 inhibited S1P-stimulated ERM phosphorylation in a dose-dependent manner such that 1μM JTE-013 notably inhibited S1P-mediated phospho-ERM while substantial inhibition was seen with 10 μM JTE-013 (Fig 4D) indicating that S1P2R plays a pivotal role in ERM phosphorylation by exogenous S1P, as well as endogenously-generated S1P (supplemental figure 5). Interestingly, S1P2R-specific inhibition prevented S1P-mediated ERM phosphorylation in U87 glioblastoma cells as well (supplemental figure 6). In addition, we examined the role of S1P2R in endogenously generated S1P-induced phospho-ERM. As described previously, HeLa cells were pretreated with vehicle or 5 μM S1P2R-specific antagonist Therefore, these results suggest that ERM phosphorylation by S1P occurs independently of the S1P1R, S1P3R, S1P4R and S1P5R while S1P2R is essential for endogenously generated or exogenously added S1P-induced phospho-ERM.

In order to further solidify S1P2R as the receptor via which S1P mediates ERM phosphorylation, HeLa cells were treated with siRNA against the S1P2R followed by S1P treatment. As seen in figure 5A, cells pretreated with control siRNA responded to 10nM S1P with robust ERM and ERK phosphorylation. On the other hand, cells pretreated with S1P2R siRNA responded notably less to S1P with a significant decrease in both ERM and ERK phosphorylation; these results support the above data (Fig 4D) that S1P2R is necessary for ERM phosphorylation in response to S1P under these conditions. To evaluate the role of S1P2R in ERM phosphorylation mediated by endogenously generated S1P, cells were treated with siRNA for S1P2R and increasing concentrations of sphingosine were added (Fig 5B). S1P2R siRNA was able to significantly inhibit sphingosine-mediated phospho-ERM, further suggesting a role for S1P2R in endogenously generated S1P-induced ERM phosphorylation (Fig 5B). Finally to consolidate the role of S1P2R in ERM phosphorylation, cell lines derived from mouse embryonic fibroblasts (MEFs), which were WT (+/+), heterozygous (−/+) or homozygous negative (−/−) for the S1P2R receptor were established. Just as in HeLa cells, MEFs were starved overnight and treated with 10 nM S1P for 10 minutes. Following S1P treatment, WT and heterozygous MEFs exhibited a robust phosphorylation of ERM; however, the S1P2R knockout MEFs showed a significantly abrogated response to S1P treatment (Fig 5C). These finding further solidify S1P2R as the receptor through which S1P induces ERM activation.

Lastly, and in addition to the above techniques, using a GFP-tagged S1P2R construct, S1P2R activation and internalization upon S1P treatment was examined. HeLa cells were transfected with 1 μg S1P2R-GFP plasmid and exposed to S1P in the presence or absence of 5 μM JTE-013. Following fixation, receptor localization was visualized using confocal microscopy. In control, untreated cells, S1P2R remained primarily at the plasma membrane with little recycling observed (Fig 6A). On the other hand, after treatment with 100 nM S1P for 5 minutes, the amount of receptor on the membrane decreased and very small punctate spots in the cytosol became visible; indicative of S1P2R activation and internalization (Fig 6B). In line with acute activation (as early as 30 seconds) of ERM proteins by S1P, receptor internalization is observed as early as 30 seconds following treatment with exogenous S1P (supplemental figure 7A). Moreover, S1P2R internalization occurs in an SK-dependent manner, such that in the presence of SKi-II, sphingosine was unable to induce receptor internalization (supplemental figure 7B). In line with the above observations, cells pretreated with S1P2R antagonist showed substantially less receptor internalization with S1P treatment

(Fig 6C). These data provide strong pharmacologic, genetic and visual evidence for S1P2R involvement in S1P-mediated ERM phosphorylation

S1P induces filopodia formation via S1P2R-dependent ERM phosphorylation

Given the data described above, it became necessary for us to determine the mechanism by which S1P-mediated pERM-dependent filopodia formation occurs. In order to address this, we used a pharmacological approach to examine the involvement of S1P receptors in S1P-induced pERM-required filopodia formation. As described above, we treated HeLa cells with FTY720-P and examined cytoskeletal rearrangements, including filopodia formation. Briefly, 10 nM FTY720-P was added to cells for 10 minutes, cells were then fixed, permeabilized and stained for F-actin (phalloidin, red), phospho-ERM (green) and nuclei (DRAQ5, blue). No changes in ERM phosphorylation or cellular morphology, including filopodial protrusions, were seen in cells exposed to FTY720-P (Fig 7D). These results are in line with the above observations (Fig 4A) suggesting that FTY720-P is unable to induce ERM phosphorylation. Next, we examined the role of S1P2R in S1P-induced pERM-mediated filopodia formation. As seen in Figure 6A, untreated HeLa cells showed punctate low-level cytoplasmic expression of phospho-ERM. S1P induced a robust and rapid increase in ERM phosphorylation and localization to newly formed cellular processes (Fig 6B); however, treating cells with FTY720-P did not (Fig 7C). Pretreating cells for 1 hour with 1 μM S1P2R-specific antagonist, JTE-013, abrogated S1P-induced ERM phosphorylation (shown via western blot in figure 4D and with confocal microscopy in Fig 7D), as well as S1P-mediated filopodia formation (Fig 7D). These data highlight the role of S1P2R in S1P-mediated ERM activation and filopodia formation.

Inhibition of S1P2R induces cellular invasion

Lastly, and in order to determine the role of S1P2R-dependent, S1P-induced ERM activation and filopodia formation in metastatic behavior, we examined the invasiveness of cells in response to S1P in the presence or absence of S1P2R-specific inhibitor, JTE-013. Using matrigel-coated trans well dishes, we examined cellular invasion toward complete media (CM), serum free media (SF) or SF media containing 500nM S1P. HeLa cells were serum starved for 4–6 hours, trypsinized and washed with serum free media before plating. 100,000 cells in SF media or SF media containing 5 μM JTE-013 were then added to the apical chamber of the trans well system and cells were allowed to invade for 48h. Following 48h, cells were stained and counted. As expected, significant cellular invasion was observed toward complete media, while little to no invasion occurred toward SF media in the presence or absence of JTE-013 (Fig 8). Interestingly, SF media containing S1P was unable to induce invasion above that of SF media, suggesting that S1P-activation of ERM proteins and subsequent filopodia formation does not lead to cellular invasion (Fig 8). On the other hand, cells exposed to S1P2R antagonist significantly invaded toward S1P, suggesting that inhibition of S1P2R promotes invasion toward S1P (Fig 8). These data in concert with the previously presented data provide insight into the mechanism by which S1P-induces filopodia formation and inhibition of invasion: through S1P2R-dependent phosphorylation of ERM proteins.

Discussion

In this manuscript we describe the mechanism of S1P-induced, ERM-dependent filopodia formation. Exogenously-added or endogenously-generated S1P was sufficient to induce robust ERM phosphorylation. Functionally, S1P induced cytoskeletal remodeling, more explicitly, the formation of cellular protrusions and filopodia, in a process that required activation of ERM proteins by phosphorylation of the C-terminal threonine residue. Using numerous approaches, we show that S1P-induced, pERM-mediated filopodia formation

occurs through activation specifically of S1P2R. Collectively, our results characterize a novel pathway in which SK/S1P regulates changes in cellular architecture that require S1P2R and subsequent phosphorylation of ERM proteins.

S1P-induced cytoskeletal rearrangement is dependent on ERM phosphorylation

S1P has been shown to govern many mechanical properties of the cell, such as regulation of cortical actin assembly and consequent lamellipodial protrusion formation [34, 35]; however, the mechanisms have remained elusive. In this study, we found that S1P treatment induced vast changes in cell structure with an abundance of cytoskeletal protrusions. Although less well-characterized serine and tyrosine ERM phosphorylation sites have been identified [18, 36], the C-terminal threonine residue (ezrin 567, radixin 564, moesin 558) is known to be the phosphorylation site required for ERM activation. Using the T567A non-phosphorylatable ezrin mutant, we provide evidence that S1P leads to phosphorylation of this specific site and that this C-terminal phosphorylation is required for S1P-induced filopodia formation. The T567A ezrin mutant not only failed to translocate to membrane protrusions but also prevented their formation following S1P treatment, thus functioning as a dominant negative. Our previous work has identified sphingolipids as regulators of ERM [1]; furthermore, we have identified a direct cellular biological process induced by sphingolipids requiring the activation of ERM proteins.

S1P2R is required for S1P-induced phospho-ERM

Using a variety of pharmacological reagents, such as specific agonists and antagonists of S1P receptors, siRNA and genetic knockouts, we demonstrate that S1P2R is the predominant receptor involved in mediating the effects of S1P on ERM phosphorylation. Initially, the short time and low dose required for ERM phosphorylation in our study strongly suggests a S1P receptor-mediated response, similar to that of acute S1PR-mediated calcium release in lung epithelial cells, which occurs as early as 20 seconds after S1P treatment [37] FTY720-P, which acts as an agonist to receptors 1, 3, 4 and 5, was unable to induce phosphorylation of ERM, suggesting that these receptors are not involved in S1P-induced phospho-ERM. Also, the receptor expression profile of the MEFs used in the current study revealed no detectable expression of S1P4R or S1P5R, suggesting that the S1P-mediated phospho-ERM signal in these cells is unlikely to be through activation of S1P4R or S1P5R. Activation of S1P1R with SEW-2871 did not induce ERM phosphorylation; likewise, selective inhibition of S1P3R did not prevent S1P-mediated phospho-ERM. Moreover, down regulation of S1P2R with siRNA and the use of S1P2R null MEFs consolidated our conclusion by showing inhibition of ERM phosphorylation following sphingosine or S1P treatment. Alternatively, minor contributions from other less well characterized S1P receptors cannot be conclusively excluded by the approaches used. Importantly, S1P-induced phospho-ERM is not cell-type specific as we were able to show ERM phosphorylation in a plethora of cell types including breast and lung cancer cells, glioblastoma cells, chondrogenic cells and fibroblasts (supplemental figure 8). In addition, we were able to identify S1P2R as the necessary receptor in U-87 glioblastoma cells, suggesting that the involvement of S1P2R in S1P-mediated phospho-ERM is also not cell-type specific (supplemental figure 6). Based on these observations, we conclude that S1P activates ERM proteins via S1P2R and speculate that this may be one of the main functions of S1P2R because of the robust and rapid manner in which it occurs.

Interestingly and in contrast to the role of S1P2R in mediating S1P effects on ERMs and membrane protrusions, it does not appear to be involved in mediating the effects of S1P on stress fiber formation. [38]. Thus, while FTY720-P was unable to promote formation of cellular processes, it did induce the formation of stress fibers (data not shown), suggesting that FTY720-P functions similarly to S1P in the formation of stress fibers yet not in

promotion of cellular protrusions. Therefore, it appears that distinct S1P receptors are required for regulating protrusions versus stress fiber formation. Since ERM proteins have been well documented to induce cell migration, we were surprised to find that ERM proteins are phosphorylated via S1P2R. S1P2R has been described as an inhibitor of migration, leaving us curious about the function of S1P2R-mediated phospho-ERM. In the current study, S1P-induced ERM activation and filopodia formation did not lead to cellular invasion; in fact, S1P signaling via S1P2R prevented cellular invasion such that S1P2R inhibition promoted invasion. This is in line with previous studies suggesting that S1P2R blocks S1P-induced invasion and migration. Additional studies examining the role of S1P in the differential regulation of ERM proteins in basal versus pathological conditions will be necessary in order to fully understand the interplay between the two.

Implications

The results from our study have many important biological implications. ERM proteins and S1P share several cellular roles, including organization of architecture and formation of structures such as lamellipodia and filopodia which are known to influence subsequent adhesion, migration, invasion, survival and proliferation [2, 39–41].

The current results have important implications to cancer including tumor progression, metastasis and perhaps evasion from apoptosis. Much is known about the involvement of the SK/S1P pathway in various stages of cancer [42]. First, SK has been implicated in initiation of cancer by its ability to function as a Ras-dependent oncogene [43]. As previously mentioned, the SK/S1P pathway plays a major role in inflammation which is beginning to be linked to certain types of cancers [44]. S1P has been associated with cancer maintenance through its pro-growth and survival properties [45, 46], as well as cancer progression through its cell migratory functions. Remarkably, ERM proteins have been implicated in most all of the aforementioned processes. ERM proteins have been shown to be overexpressed in some cancers, positively correlating with cancer cell survival, proliferation, migration, adhesion and invasion. The current results provide a more specific link between S1P, ERM phosphorylation and filopodial formation. We put forth the idea that phosphorylation of ERM is perhaps a major mechanism by which the SK/S1P pathway contributes to cancer cell development and metastasis.

While the data in this study suggests that S1P signaling via S1P2R inhibits invasion, we suggest that global activation of ERM, around the entire periphery of the cell, leads to increased cell-cell adhesion such as that which occurs in epithelial sheet formation. Filopodia formation has been shown to promote cell-cell contacts and induce a phenomenon known as “adhesion zippering,” whereby, formation of mature adherens junctions by interdigitated filopodia from neighboring cells align and adhere cells, in a calcium-dependent manner [47, 48]. Interestingly, S1P2R has been linked to calcium mobilization in overexpression studies [49], as well as in knockout studies [50]. This data is complementary to the findings that S1P promotes endothelial barrier function via regulation of ERM proteins [51]. Further exploration of the role of S1P/S1P2R in the formation of cell-cell adhesions may prove useful in the area of wound healing. In contrast to its role in the inhibition of invasion, there is evidence suggesting that S1P2R actually contributes to cancer progression and metastasis by enhancing cell adhesion and subsequent invasion [39]. It will be interesting to explore the role of ligand-induced activation of SK and subsequent regulation of ERM proteins. Perhaps ligand induced cellular polarization, such as that which occurs with various chemo attractants, and localized activation of the SK/S1P pathway leads to asymmetrical activation of ERM proteins, driving cell migration and/ or invasion. The cellular localization of S1P2R indubitably affects the outcome of its activation, and this may account for the controversy surrounding the role of S1P2R in cellular invasion and migration.

In lymphocyte biology, many of the aforementioned biologies are important components of inflammation and immunity, particularly with regard to migrating lymphocytes. For example, S1P is known to be involved in lymphocyte egress, chemotaxis, and homing through S1P1R mediated migration, such that down regulation of S1P1R results in lymphopenia [52, 53]. Interestingly, ERM proteins have been extensively studied in the polarization and migration of lymphocytes [54]. Phosphorylated ezrin has been shown to localize to the rear of EL4.G8 T-lymphoma cells during chemotaxis and this rear localization of phospho-ezrin may potentially function in retraction of the lagging edge of the cell [55]. In that study, T-cells expressing the T567D phosphomimetic ezrin mutant had significantly larger trailing protrusions compared to cells expressing wild type ezrin and T567A non-phosphorylatable ezrin mutant [56]. On the other hand, phosphorylated ERM proteins have also been shown to localize to lamellipodia at the leading edge of B-lymphoma cells to promote forward protrusion [57]. Whether at the leading or lagging edge of lymphocytes, ERM proteins have been shown to play a major role in lymphocyte polarization, chemotaxis and homing providing overlapping functions of S1P and ERM proteins.

Another intriguing direct connection emerges in cochlear function. Maintenance of cell junctions is an important function of both S1P and ERM proteins, and this is highlighted best in the preservation of cochlear integrity. Mice null for the S1P2R receptor exhibit a progressive hearing loss phenotype and are deaf by one month of age due to deterioration in the barrier epithelium of the cochlea [58, 59]; interestingly, radixin knockout mice also experience deafness due to improper structural maintenance of cochlear stereocilia [58, 60]. Thus, the current results establishing S1P as a potent and robust inducer of ERM phosphorylation raised the intriguing possibility that ERM regulation may be a major function of the SK/S1P pathway in the cochlea.

Additionally, both S1P and ERM proteins have been implicated in neovasculogenesis, angiogenesis and vascular function and constitute another example of how S1P and ERM proteins may coordinate and/or share biological functions. Specifically, SK1/SK2 double knockout mice and S1P1R knockout mice die by embryonic day 13.5 due hemorrhage brought on by improper blood vessel formation [61]; remarkably, ERM proteins play a major role in promoting endothelial cell polarity, cell migration, *in vivo* lumen formation, cell-cell adhesion and endothelial barrier function [2] providing compelling evidence of an additional fundamental S1P-dependent biology which may be mediated by ERM proteins.

Lastly, these results reveal potential novel therapeutic targets for the treatment of cancer, inflammation and other diseases involving deregulation of SK/S1P and/or ERM proteins. The SK/S1P pathway is essential to life as evidenced by the lethality of SK1/SK2 and S1P1R gene knockout in mice. There has yet to be a triple knockout of ezrin, radixin and moesin; however, given the number of important cellular processes in which they are involved, it is likely that devastating phenotypes would be observed. Targeting the SK/S1P pathway therapeutically has proven to be difficult in that the basal, homeostatic functions carried out by SK/S1P are affected; similarly, therapeutically targeting ERM proteins will disrupt the major normal cellular functions to which they contribute: for example spindle formation and cytokinesis [2]. Our findings that S1P-induction of phospho-ERM occurs through the S1P2R receptor expose a novel target for various therapies; specific antagonists of S1P2R currently exist and are well tolerated in animal studies [62] and knockout of the S1P2R gene in mice is not lethal [59, 63]. In conclusion, we have demonstrated a role for ERM proteins in mediating signals of the SK/S1P/S1P2R pathway and suggest that localization of S1P2R and subsequent localized activation of ERM proteins may play a role in the cellular response to S1P

Supplementary Material

Refer to Web version on PubMed Central for supplementary material.

Acknowledgments

We would like to thank all the Hannun and Obeid lab members. LC MS/MS sphingolipid analysis was carried out by the MUSC Lipidomics Shared Resource in the facility supported by NIH Grant C06 RR018823. Additionally, we thank the MUSC Cell and Molecular Imaging Core. A special thanks to Sphynx Therapeutics (Charlottesville, VA) for kindly providing the SK inhibitor, SKX. Lastly, we thank Kathy Wiita-Fisk for her administrative assistance and Christopher J. Clarke, Ph.D. for his editorial assistance.

This manuscript is based upon work supported in part by a MERIT Award, [BX000156-01A1] (L.M.O.) by the Office of Research and Development, Department of Veterans Affairs, Ralph H. Johnson VA Medical Center, Charleston, South Carolina. The content of this material does not represent the views of the Department of Veterans Affairs or the United State Government; US Department of Education Graduate Assistance in Areas of National Need (GAANN) in Lipid Biology and New Technologies, [P200A070596] (K.A.O.G.); and National Institutes of Health grants [HL-007260] (K.A.O.G.), National Cancer Institute [R01-CA87584 (Y.A.H.), PO1-CA97132 (Y.A.H. and L.M.O.)] and National Institutes of Health National Institute of General Medical Sciences [R01-GM062887 (L.M.O.)]. The imaging facilities for this research were supported, in part, by Cancer Center Support Grant [P30 CA138313] to the Hollings Cancer Center, Medical University of South Carolina

Abbreviations

ERM	ezrin radixin and moesin
pERM	phospho-ezrin radixin and moesin
CD95	FasL receptor
NHE1	sodium hydrogen exchanger 1
NF2	merlin
PIP2	phosphatidylinositol 4, 5 bisphosphate
PKC	protein kinase C
GRK2	G protein-coupled receptor kinase 2
EGF	epidermal growth factor
PDGF	platelet-derived growth factor
S1P	sphingosine 1-phosphate
SK1	sphingosine kinase 1
SK2	sphingosine kinase 2
GPCR	G protein-coupled receptor
S1P1R-S1P5R	sphingosine 1-phosphate receptor 1–5
sph	sphingosine
NEO	neomycin
ERK	extracellular regulated kinase
pERK	phospho-extracellular regulated kinase
MEFs	mouse embryonic fibroblasts
GAPDH	glyceraldehyde-3-phosphate dehydrogenase

References

1. Canals D, Jenkins RW, Roddy P, Hernandez-Corbacho MJ, Obeid LM, Hannun YA. Differential effects of ceramide and sphingosine-1-phosphate on ERM phosphorylation: probing sphingolipid signaling at the outer plasma membrane. J Biol Chem. 2010; 285(42):32476–85. [PubMed: 20679347]
2. Fehon RG, McClatchey AI, Bretscher A. Organizing the cell cortex: the role of ERM proteins. Nat Rev Mol Cell Biol. 2010; 11:276–287. [PubMed: 20308985]
3. Arpin M, Chirivino D, Naba A, Zwaenepoel I. Emerging role for ERM proteins in cell adhesion and migration. Cell Adh Migr. 2011; 5:199–206. [PubMed: 21343695]
4. Ren L, Hong SH, Cassavaugh J, Osborne T, Chou AJ, Kim SY, Gorlick R, Hewitt SM, Khanna C. The actin-cytoskeleton linker protein ezrin is regulated during osteosarcoma metastasis by PKC. Oncogene. 2009; 28:792–802. [PubMed: 19060919]
5. He ZY, Wen H, Shi CB, Wang J. Up-regulation of hnRNP A1, Ezrin, tubulin beta-2C and Annexin A1 in sentinel lymph nodes of colorectal cancer. World J Gastroenterol. 2010; 16:4670–4676. [PubMed: 20872967]
6. Li J, Tu Y, Wen J, Yao F, Wei W, Sun S. Role for ezrin in breast cancer cell chemotaxis to CCL5. Onc Reports. 2010; 24:965–971.
7. Parlato S, Giammarioli AM, Logozzi M, Lozupone F, Matarrese P, Luciani F, Falchi M, Malorni W, Fais S. CD95 (APO-1/Fas) linkage to the actin cytoskeleton through ezrin in human T lymphocytes: a novel regulatory mechanism of the CD95 apoptotic pathway. EMBO J. 2000; 19:5123–5134. [PubMed: 11013215]
8. Harrison GM, Davies G, Martin TA, Jiang WG, Mason MD. Distribution and expression of CD44 isoforms and Ezrin during prostate cancer-endothelium interaction. Int J Oncol. 2002; 21:935–940. [PubMed: 12370738]
9. Chiang Y, Chou CY, Hsu KF, Huang YF, Shen MR. EGF upregulates Na+/H+ exchanger NHE1 by post-translational regulation that is important for cervical cancer cell invasiveness. J Cell Physiol. 2008; 214:810–819. [PubMed: 17894388]
10. Elliott BE, Meens JA, SenGupta SK, Louvard D, Arpin M. The membrane cytoskeletal crosslinker ezrin is required for metastasis of breast carcinoma cells. Breast Can Res. 2005; 7:R365–373.
11. Takada Y, Ye X, Simon S. The integrins. Genome Biol. 2007; 8:215. [PubMed: 17543136]
12. Chen Y, Wang D, Guo Z, Zhao J, Wu B, Deng H, Zhou T, Xiang H, Gao F, Yu X, Liao J, Ward T, Xia P, Emenari C, Ding X, Thompson W, Ma K, Zhu J, Aikhionbare F, Dou K, Cheng SY, Yao X. Rho kinase phosphorylation promotes ezrin-mediated metastasis in hepatocellular carcinoma. Can Res. 2011; 71:1721–1729.
13. Boldrini E, Peres SV, Morini S, de Camargo B. Immunoexpression of Ezrin and CD44 in patients with osteosarcoma. J Pediatr Hematol Oncol. 2010; 32:e213–217. [PubMed: 20562647]
14. Estecha A, Sanchez-Martin L, Puig-Kroger A, Bartolome RA, Teixido J, Samaniego R, Sanchez-Mateos P. Moesin orchestrates cortical polarity of melanoma tumour cells to initiate 3D invasion. J Cell Sci. 2009; 122:3492–3501. [PubMed: 19723803]
15. Kahsai AW, Zhu S, Fenteany G. G protein-coupled receptor kinase 2 activates radixin, regulating membrane protrusion and motility in epithelial cells. BBA. 2010; 1803:300–310. [PubMed: 19913059]
16. Nakamura N, Oshiro N, Fukata Y, Amano M, Fukata M, Kuroda S, Matsuura Y, Leung T, Lim L, Kaibuchi K. Phosphorylation of ERM proteins at filopodia induced by Cdc42. Genes to cells. 2000; 5:571–581. [PubMed: 10947843]
17. Baumgartner M, Sillman AL, Blackwood EM, Srivastava J, Madson N, Schilling JW, Wright JH, Barber DL. The Nck-interacting kinase phosphorylates ERM proteins for formation of lamellipodium by growth factors. PNAS. 2006; 103:13391–13396. [PubMed: 16938849]
18. Gould KL, Cooper JA, Bretscher A, Hunter T. The protein-tyrosine kinase substrate, p81, is homologous to a chicken microvillar core protein. J Cell Biol. 1986; 102:660–669. [PubMed: 2418035]
19. Zeidan YH, Jenkins RW, Hannun YA. Remodeling of cellular cytoskeleton by the acid sphingomyelinase/ceramide pathway. J Cell Biol. 2008; 181:335–350. [PubMed: 18426979]

20. Hannun YA, Obeid LM. Principles of bioactive lipid signalling: lessons from sphingolipids. Nat Rev Mol Cell Biol. 2008; 9:139–150. [PubMed: 18216770]
21. Kawamori T, Osta W, Johnson KR, Pettus BJ, Bielawski J, Tanaka T, Wargovich MJ, Reddy BS, Hannun YA, Obeid LM, Zhou D. Sphingosine kinase 1 is up-regulated in colon carcinogenesis. FASEB J. 2006; 20:386–388. [PubMed: 16319132]
22. Jenkins RW, Clarke CJ, Canals D, Snider AJ, Gault CR, Heffernan-Stroud L, Wu BX, Simbari F, Roddy P, Kitatani K, Obeid LM, Hannun YA. Regulation of CC ligand 5/RANTES by acid sphingomyelinase and acid ceramidase. J Biol Chem. 2011; 286:13292–13303. [PubMed: 21335555]
23. Sato K, Ishikawa K, Ui M, Okajima F. Sphingosine 1-phosphate induces expression of early growth response-1 and fibroblast growth factor-2 through mechanism involving extracellular signal-regulated kinase in astroglial cells. Brain Res Mol Brain Res. 1999; 74:182–189. [PubMed: 10640689]
24. Alderton F, Darroch P, Sambi B, McKie A, Ahmed IS, Pyne N, Pyne S. G-protein-coupled receptor stimulation of the p42/p44 mitogen-activated protein kinase pathway is attenuated by lipid phosphate phosphatases 1, 1a, and 2 in human embryonic kidney 293 cells. J Biol Chem. 2001; 276:13452–13460. [PubMed: 11278307]
25. Tolan D, Conway AM, Rakhit S, Pyne N, Pyne S. Assessment of the extracellular and intracellular actions of sphingosine 1-phosphate by using the p42/p44 mitogen-activated protein kinase cascade as a model. Cell Signal. 1999; 11:349–354. [PubMed: 10376808]
26. Kharel Y, Mathews TP, Gellett AM, Tomsig JL, Kennedy PC, Moyer ML, Macdonald TL, Lynch KR. Sphingosine kinase type 1 inhibition reveals rapid turnover of circulating sphingosine 1-phosphate. Biochem J. 2011; 440:345–353. [PubMed: 21848514]
27. Canals D, Jenkins RW, Roddy P, Hernandez-Corbacho MJ, Obeid LM, Hannun YA. Differential effects of ceramide and sphingosine 1-phosphate on ERM phosphorylation: probing sphingolipid signaling at the outer plasma membrane. J Biol Chem. 2010; 285:32476–32485. [PubMed: 20679347]
28. Simons PC, Pietromonaco SF, Reczek D, Bretscher A, Elias L. C-terminal threonine phosphorylation activates ERM proteins to link the cell's cortical lipid bilayer to the cytoskeleton. Biochem Biophys Res Commun. 1998; 253:561–565. [PubMed: 9918767]
29. Gautreau A, Louvard D, Arpin M. Morphogenic effects of ezrin require a phosphorylation-induced transition from oligomers to monomers at the plasma membrane. J Cell Biol. 2000; 150:193–203. [PubMed: 10893267]
30. Osinde M, Mullershausen F, Dev KK. Phosphorylated FTY720 stimulates ERK phosphorylation in astrocytes via S1P receptors. Neuropharm. 2007; 52:1210–1218.
31. Awad AS, Ye H, Huang L, Li L, Foss FW Jr, Macdonald TL, Lynch KR, Okusa MD. Selective sphingosine 1-phosphate 1 receptor activation reduces ischemia-reperfusion injury in mouse kidney. Am J Physiol Renal Physiol. 2006; 290:F1516–1524. [PubMed: 16403835]
32. Laychock SG, Sessanna SM, Lin MH, Mastrandrea LD. Sphingosine 1-phosphate affects cytokine-induced apoptosis in rat pancreatic islet beta-cells. Endocrinology. 2006; 147:4705–4712. [PubMed: 16794003]
33. Arikawa K, Takuwa N, Yamaguchi H, Sugimoto N, Kitayama J, Nagawa H, Takehara K, Takuwa Y. Ligand-dependent inhibition of B16 melanoma cell migration and invasion via endogenous S1P2 G protein-coupled receptor. Requirement of inhibition of cellular RAC activity. J Biol Chem. 2003; 278:32841–32851. [PubMed: 12810709]
34. Maceyka M, Alvarez SE, Milstien S, Spiegel S. Filamin A links sphingosine kinase 1 and sphingosine-1-phosphate receptor 1 at lamellipodia to orchestrate cell migration. Mol Cell Biol. 2008; 28:5687–5697. [PubMed: 18644866]
35. Klausen C, Leung PC, Auersperg N. Cell motility and spreading are suppressed by HOXA4 in ovarian cancer cells: possible involvement of beta1 integrin. Mol Can Res. 2009; 7:1425–1437.
36. Bretscher A. Rapid phosphorylation and reorganization of ezrin and spectrin accompany morphological changes induced in A-431 cells by epidermal growth factor. J Cell Biol. 1989; 108:921–930. [PubMed: 2646308]

37. Chen LY, Woszczek G, Nagineni S, Logun C, Shelhamer JH. Cytosolic phospholipase A2alpha activation induced by S1P is mediated by the S1P3 receptor in lung epithelial cells. Am J Physiol Lung Cell Mol Physiol. 2008; 295:L326–335. [PubMed: 18502815]
38. Formigli L, Meacci E, Sassoli C, Chellini F, Giannini R, Quercioli F, Tiribilli B, Squecco R, Bruni P, Francini F, Zecchi-Orlandini S. Sphingosine 1-phosphate induces cytoskeletal reorganization in C2C12 myoblasts: physiological relevance for stress fibres in the modulation of ion current through stretch-activated channels. J Cell Sci. 2005; 118:1161–1171. [PubMed: 15728255]
39. Young N, Van Brocklyn JR. Roles of sphingosine-1-phosphate (S1P) receptors in malignant behavior of glioma cells. Differential effects of S1P2 on cell migration and invasiveness. Exp Cell Res. 2007; 313:1615–1627. [PubMed: 17376432]
40. Torer N, Kayaselcuk F, Nursal TZ, Yildirim S, Tarim A, Noyan T, Karakayali H. Adhesion molecules as prognostic markers in pancreatic adenocarcinoma. J Surg Oncol. 2007; 96:419–423. [PubMed: 17874463]
41. Donati C, Bruni P. Sphingosine 1-phosphate regulates cytoskeleton dynamics: implications in its biological response. BBA. 2006; 1758:2037–2048. [PubMed: 16890187]
42. Pyne NJ, Pyne S. Sphingosine 1-phosphate and cancer. Nat Rev Can. 2010; 10:489–503.
43. Xia P, Gamble JR, Wang L, Pitson SM, Moretti PA, Wattenberg BW, D'Andrea RJ, Vadas MA. An oncogenic role of sphingosine kinase. Curr Biol. 2000; 10:1527–1530. [PubMed: 11114522]
44. Swann JB, Vesely MD, Silva A, Sharkey J, Akira S, Schreiber RD, Smyth MJ. Demonstration of inflammation-induced cancer and cancer immunoediting during primary tumorigenesis. PNAS. 2008; 105:652–656. [PubMed: 18178624]
45. Xia P, Wang L, Gamble JR, Vadas MA. Activation of sphingosine kinase by tumor necrosis factor-alpha inhibits apoptosis in human endothelial cells. J Biol Chem. 1999; 274:34499–34505. [PubMed: 10567432]
46. Pitson SM. Regulation of sphingosine kinase and sphingolipid signaling. Trends in Biochem Sci. 2011; 36:97–107. [PubMed: 20870412]
47. Vasioukhin V, Bauer C, Yin M, Fuchs E. Directed actin polymerization is the driving force for epithelial cell-cell adhesion. Cell. 2000; 100:209–219. [PubMed: 10660044]
48. Mattila PK, Lappalainen P. Filopodia: molecular architecture and cellular functions. Nat Rev Mol. 2008; 9:446–454.
49. Ancellin N, Hla T. Differential pharmacological properties and signal transduction of the sphingosine 1-phosphate receptors EDG-1, EDG-3, and EDG-5. J Biol Chem. 1999; 274:18997–19002. [PubMed: 10383399]
50. Ishii I, Ye X, Friedman B, Kawamura S, Contos JJ, Kingsbury MA, Yang AH, Zhang G, Brown JH, Chun J. Marked perinatal lethality and cellular signaling deficits in mice null for the two sphingosine 1-phosphate (S1P) receptors, S1P(2)/LP(B2)/EDG-5 and S1P(3)/LP(B3)/EDG-3. J Biol Chem. 2002; 277:25152–25159. [PubMed: 12006579]
51. Adyshev DM, Moldobaeva NK, Elangovan VR, Garcia JG, Dudek SM. Differential involvement of ezrin/radixin/moesin proteins in sphingosine 1-phosphate-induced human pulmonary endothelial cell barrier enhancement. Cell Signal. 2011; 23:2086–2096. [PubMed: 21864676]
52. Chiba K, Matsuyuki H, Maeda Y, Sugahara K. Role of sphingosine 1-phosphate receptor type 1 in lymphocyte egress from secondary lymphoid tissues and thymus. Cell Mol Immunol. 2006; 3:11–19. [PubMed: 16549044]
53. Oo ML, Thangada S, Wu MT, Liu CH, Macdonald TL, Lynch KR, Lin CY, Hla T. Immunosuppressive and anti-angiogenic sphingosine 1-phosphate receptor-1 agonists induce ubiquitinylation and proteasomal degradation of the receptor. J Biol Chem. 2007; 282:9082–9089. [PubMed: 17237497]
54. del Pozo MA, Vicente-Manzanares M, Tejedor R, Serrador JM, Sanchez-Madrid F. Rho GTPases control migration and polarization of adhesion molecules and cytoskeletal ERM components in T lymphocytes. Euro J Immunol. 1999; 29:3609–3620.
55. Li J, Yang H, Zhang S, Yu N, Zhou Q. Expression and their significance of ezrin and E-cadherin in non-small cell lung cancer. Zhongguo Fei Ai Za Zhi. 2007; 10:183–187. [PubMed: 21118642]

56. Li Y, Harada T, Juang YT, Kyttaris VC, Wang Y, Zidanic M, Tung K, Tsokos GC. Phosphorylated ERM is responsible for increased T cell polarization, adhesion, and migration in patients with systemic lupus erythematosus. J Immunol. 2007; 178:1938–1947. [PubMed: 17237445]
57. Parameswaran N, Matsui K, Gupta N. Conformational switching in ezrin regulates morphological and cytoskeletal changes required for B cell chemotaxis. J Immunol. 2011; 186:4088–4097. [PubMed: 21339367]
58. Kitajiri S, Fukumoto K, Hata M, Sasaki H, Katsuno T, Nakagawa T, Ito J, Tsukita S. Radixin deficiency causes deafness associated with progressive degeneration of cochlear stereocilia. J Cell Biol. 2004; 166:559–570. [PubMed: 15314067]
59. MacLennan AJ, Benner SJ, Andringa A, Chaves AH, Rosing JL, Vesey R, Karpman AM, Cronier SA, Lee N, Erway LC, Miller ML. The S1P2 sphingosine 1-phosphate receptor is essential for auditory and vestibular function. Hear Res. 2006; 220:38–48. [PubMed: 16945494]
60. Pataky F, Pironkova R, Hudspeth AJ. Radixin is a constituent of stereocilia in hair cells. PNAS. 2004; 101:2601–2606. [PubMed: 14983055]
61. Limaye A, Kashyap RS, Kapley A, Galande S, Purohit HJ, Daginawala HF, Taori GM. Modulation of signal transduction pathways in lymphocytes due to sub-lethal toxicity of chlorinated phenol. Toxicol Lett. 2008; 179:23–28. [PubMed: 18486366]
62. Skoura A, Hla T. Regulation of vascular physiology and pathology by the S1P2 receptor subtype. Cardiovasc Res. 2009; 82:221–228. [PubMed: 19287048]
63. Herr DR, Chun J. Effects of LPA and S1P on the nervous system and implications for their involvement in disease. Curr Drug Targets. 2007; 8:155–167. [PubMed: 17266539]

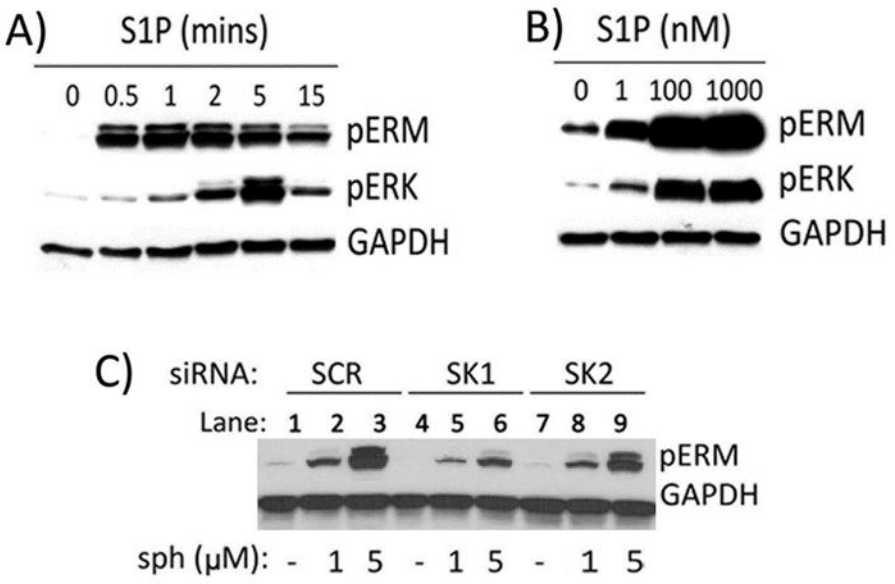

Figure 1. Effects of exogenously-added or endogenously-generated S1P on ERM phosphorylation

HeLa cells were serum starved overnight then treated with A) 100 nM S1P for the indicated times or B) for 5 minutes with the indicated doses of S1P. Phosphorylated ERM (pERM), phosphorylated ERK (pERK) and GAPDH levels were assessed via western blot. Blots are representative of n=4 experiments. C) HeLa cells were treated with 20 nM of the indicated siRNA for 48 hours. After 48 hours of siRNA, cells were serum starved 16–18 hours then treated with the indicated amounts of sphingosine for 10 minutes. Blots are representative of two experiments.

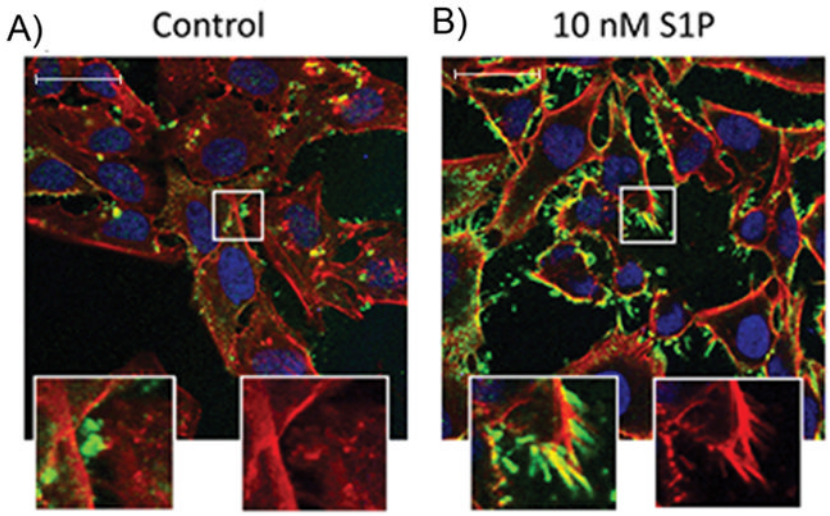

Figure 2. S1P-mediated phospho-ERM localizes to newly formed filopodia

HeLa cells were serum deprived and received no treatment (A) or were treated with (B) 10 nM S1P for 10 minutes. Cells were fixed and stained for phospho-ERM (green). Phospho-ERM, Nuclei (Draq5, blue) and F-actin (phalloidin, red) were visualized using confocal microscopy. Images showing the presence or absence of filopodia formation are enlarged in the insets. Calibration bars represent 50μm. Images are representative of at least 4 independent experiments.

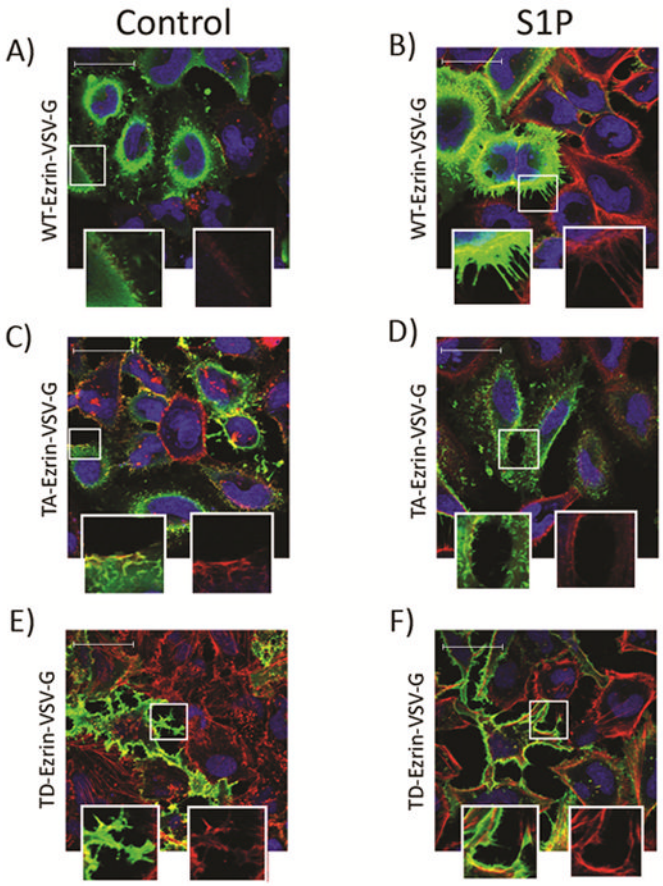

Figure 3. Requirement of phospho-ezrin in S1P-induced filopodia formation

HeLa cells were transfected with (A, B) VSV-G-tagged wild type ezrin, (C, D) VSV-G-tagged nonphoshorylatable ezrin mutant T567A or (E, F) VSV-G-tagged phospho-mimetic ezrin mutant T567D. Following transfection, cells were serum starved and received no treatment (A, C, E) or 100 nM S1P (B, D, F) treatment for 10 minutes. Cells were fixed and VSV-G (green), nuclei (DRAQ5, blue) and F-actin (phalloidin, red) were visualized using laser-scanning confocal microscopy. Calibration bars represent 50μm. Images showing the presence or absence of filopodia are enlarged in insets. Images are representative of at least 2 independent experiments.

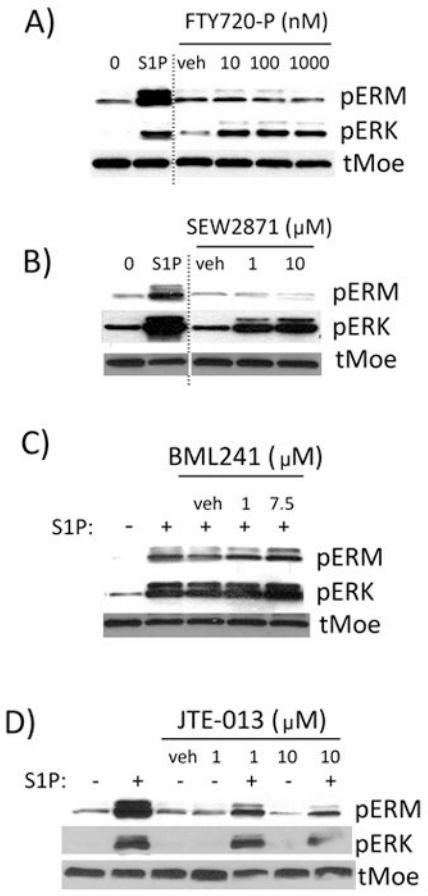

Figure 4. Effect of pharmacological modulation of S1P receptors on S1P-mediated phosphorylation of ERM proteins

HeLa cells were starved overnight and treated with A) 100 nM S1P or the indicated doses of FTY720-P (agonist for S1P1R, S1P3R, S1P4R, and S1P5R) for 10 minutes or with B) the indicated amounts of SEW-2871 (specific agonist for S1P1R) for 10 minutes. Blots are representative of two experiments. Serum starved HeLa cells were treated with 10 nM S1P for 10 minutes following 1 hour pretreatment with the indicated amounts of C) S1P3R-specific antagonist, BML-241, or D) S1P2R-specific antagonist, JTE-013. pERM, pERK and GAPDH and Moesin (tMoe) levels were analyzed via western blot. Blots representative, n=4.

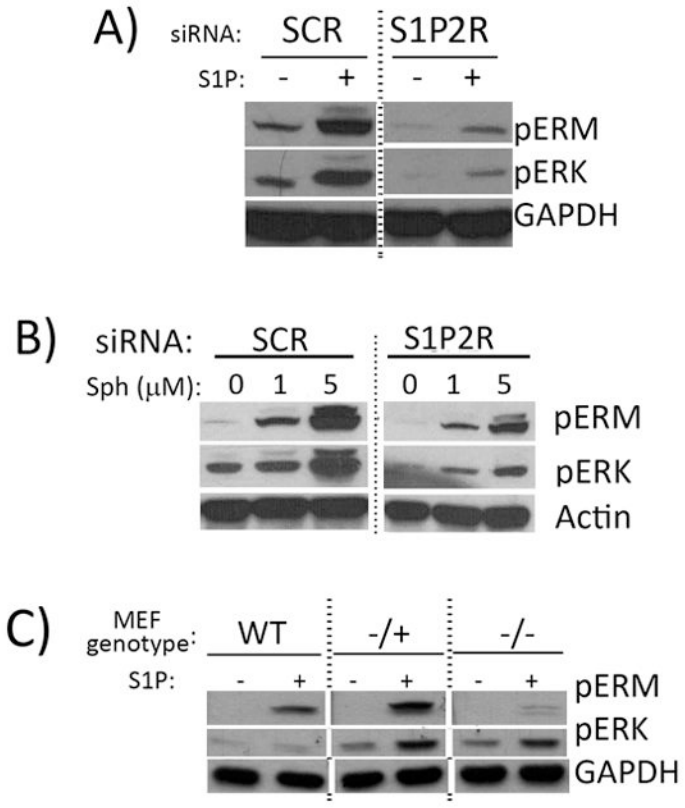

Figure 5. Effect of loss of S1P receptor 2 (S1P2R) on S1P-mediated phosphorylation of ERM proteins

HeLa cells were treated with 20 nM S1P2R siRNA for 48 hours. After 48 hours of siRNA, cells were serum starved then treated with A) 10 nM S1P or 1 μ*M or 5* μM sphingosine for 10 minutes. B) Mouse embryonic fibroblasts derived from S1P2R wild type (+/+), heterozygote (+/−) and knockout (−/−) mice were serum deprived then treated with 10 nM S1P for 10 minutes. pERM, pERK and GAPDH were analyzed via western blot. Blots representative, n=2 with two different clones for each genotype.

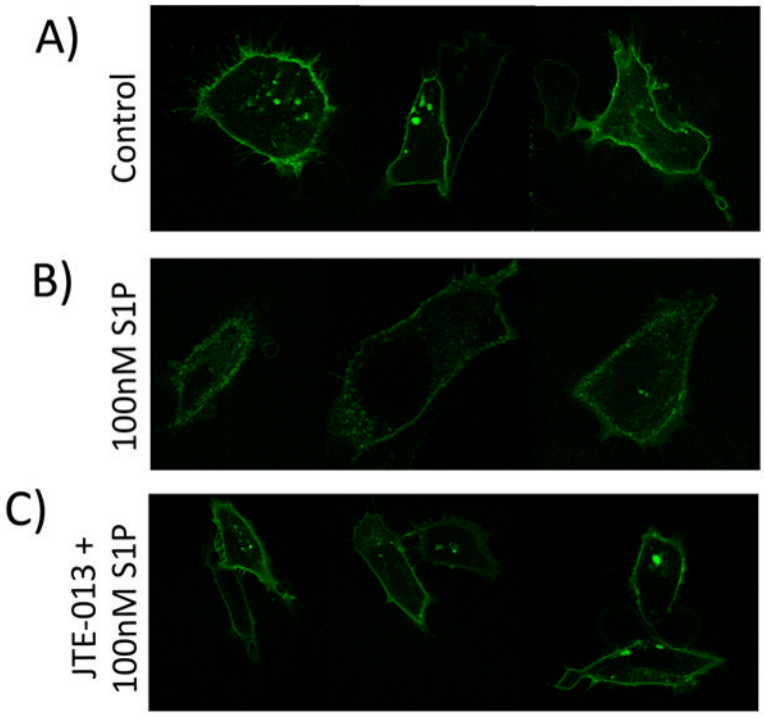

Figure 6. S1P-mediated S1P2R internalization

HeLa cells were transfected with 1μg S1P2R-GFP plasmid. 24 hours following transfection, cells were serum starved overnight. Cells were exposed to A) no treatment, B) 100 nM S1P for 5 minutes or C) 1hr pretreatment with 5 μM JTE-013 followed by 5 minutes 100 nM S1P for 5 minutes. Cells were fixed and imaged using confocal microscopy. Images are representative, $n \geq 2$

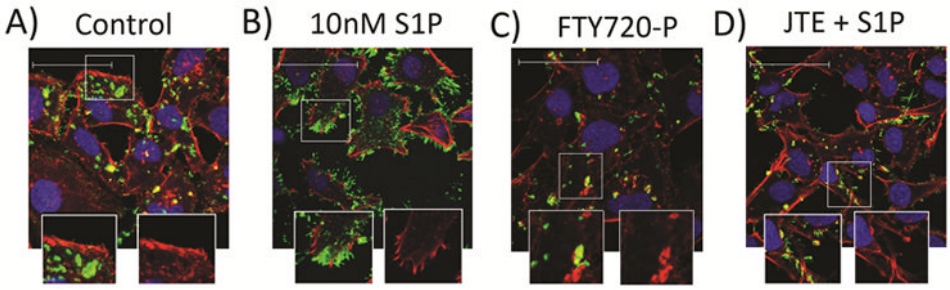

Figure 7. Effect of inhibition of S1P2R on S1P-mediated pERM and filopodia formation

HeLa cells were serum deprived and received (A) no treatment, (B) 10 nM S1P for 10 minutes, (C) 10nM FTY720-P for 10 minutes, or D) 1 hour treatment with 1 μM JTE-013, followed by 10 minutes of treatment with 10 nM S1P. Cells were fixed and phospho-ERM (green), nuclei (DRAQ5, blue) and F-actin (phalloidin, red) were visualized using confocal microscopy. Calibration bars represent 50μm. Images, showing the presence or absence of filopodia, are enlarged in insets. Images are representative of at least 2 independent experiments.

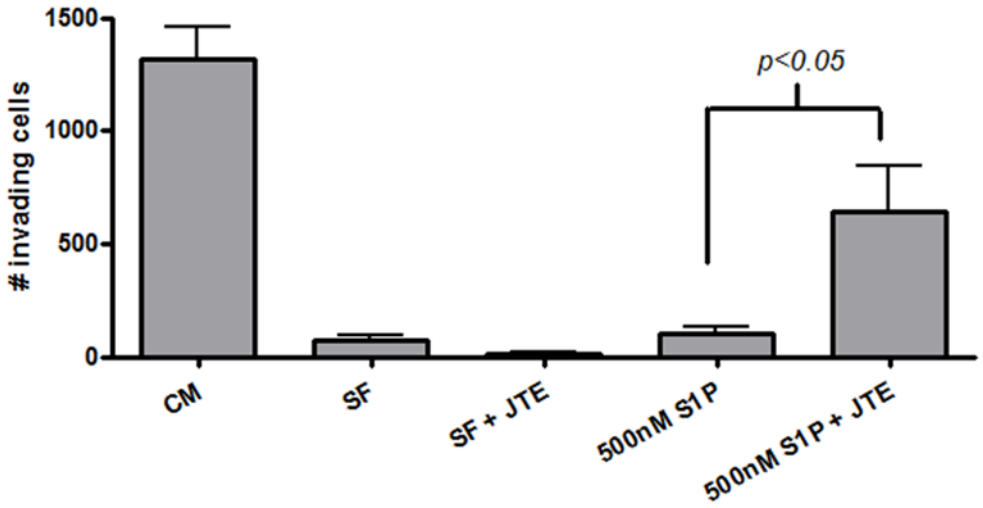

Figure 8. Role of S1P/S1P2R in cellular invasion

HeLa cells were plated, in the presence or absence of 5 μM JTE-013, in the apical chambers of matrigel coated trans well plates and allowed to invade for 48h towards complete medium (CM), serum free media (SF) or 500nM S1P. Cells were fluorescently labeled and photographed prior to counting. n ≥ 3, Student's t-test used to assess evaluate significance.